is not initiated by simple electron transfer in which low-valent dirhenium species are formed. Nonetheless, since we have recently found that nitrile ligands can be reductively coupled at the dirhenium center in $Re_2Cl_4(dppm)_2$,[26] we are currently exploring the possibility that these redox-active dimetal species may induce the reductive coupling of other organic substrates.

(26) Esjornson, D.; Fanwick, P. E.; Walton, R. A., unpublished results.

Acknowledgment. Support from the National Science Foundation, Grant No. CHE85-06702, is gratefully acknowledged.

Supplementary Material Available: Listings of anisotropic thermal parameters (Table S1), bond distances (Table S2), and bond angles (Table S3) associated with the phenyl rings and PF_6^- anion and a figure showing the full atomic numbering scheme (Figure S1) (5 pages); a table of observed and calculated structure factors (15 pages). Ordering information is given on any current masthead page.

Contribution from the Department of Inorganic Chemistry, University of Umeå, S-901 87 Umeå, Sweden, and the Department of Chemistry, Faculty of Science, The University of Tokyo, Hongo, Bunkyo-ku, Tokyo 113, Japan

Multicomponent Polyanions. 41. Potentiometric and ^{31}P NMR Study of Equilibria in the Molybdophenylphosphonate System in 0.6 M Na(Cl) Medium

Atsushi Yagasaki,*† Ingegärd Andersson,‡ and Lage Pettersson*‡

Received February 2, 1987

The equilibria in the H^+–MoO_4^{2-}–$C_6H_5PO_3^{2-}$ system have been studied by potentiometry and ^{31}P NMR spectroscopy in 0.6 M Na(Cl) medium at 25 °C. The potentiometric data covered the range $8.2 \gtrsim -\lg [H^+] \gtrsim 1.4$.[1] The NMR spectra were recorded in the range $8.7 \gtrsim -\lg [H^+] \gtrsim 0.0$. The total concentrations of molybdate, B, and phenylphosphonate, C, were varied within the limits $10 \leq B/\text{mM} \leq 80$ and $5 \leq C/\text{mM} \leq 40$ with $1 \leq B/C \leq 16$. The following ternary species, denoted by (p,q,r) according to the general formula $(H^+)_p(MoO_4^{2-})_q(C_6H_5PO_3^{2-})_r$, have been found: (10,5,2), (11,5,2), (11,7,1), (12,7,1), and (12,6,1). Values of the logarithm of the formation constants are as follows: $\lg \beta_{10,5,2} = 68.07 \pm 0.02$, $\lg \beta_{11,5,2} = 69.40 \pm 0.10$, $\lg \beta_{11,7,1} = 71.96 \pm 0.09$, $\lg \beta_{12,7,1} = 75.70 \pm 0.04$, and $\lg \delta_{12,6,1} = 69.04 \pm 0.05$. The structures of the ternary species in solution are discussed.

Introduction

In the field of solution chemistry the importance of studying a given system by more than one method has repeatedly been emphasized in the literature. However, a large number of stability constants have been determined by only one method, partly because it is often difficult to apply two or more methods to the system one is going to investigate. In equilibrium analysis potentiometry is most frequently chosen from several different methods because of its wide range of applicability and high accuracy and precision. Many stability constants have been determined just by measuring the hydrogen ion concentration with a glass electrode.

Although it is a powerful tool for investigating equilibria of simple systems, potentiometry often fails to give an unambiguous speciation for a complicated system like a polyoxometalate system, where several polynuclear species are formed. This is in spite of the fact that high-accuracy data have been collected, a constant medium background has been used, and the total concentrations and the ratios between the components have been extended as much as possible without changing the activity factors. A typical example is the molybdophosphate system, where in a recent reinvestigation by a combined emf–NMR method several new species were found, which could not be established by potentiometry alone.[2]

The equilibria in the title system are expected to be much simpler than in the molybdophosphate system, since one of the reaction sites of the heteroatom group is blocked by the organic group. In the literature only one type of organophosphonate heteropolyanion, $(RPO_3)_2Mo_5O_{15}^{n-}$, with a structure analogous to that of $(HOPO_3)_2Mo_5O_{15}^{4-}$,[3] has been reported.[4,5] As some preliminary experiments at our department showed the existence of two or more heteropoly species in solution, we decided to make a thorough study of the system.

In the present paper we report the result of the equilibrium analysis of the molybdophenylphosphonate system based on both potentiometric and ^{31}P NMR data in 0.6 M Na(Cl) medium. The combined emf–NMR data were evaluated by using a new computer program, LAKE, which was developed in parallel with the current study.

Symbols

The equilibria of the title system can be written in the general form

$$p\mathrm{H}^+ + q\mathrm{MoO_4}^{2-} + r\mathrm{C_6H_5PO_3}^{2-} \rightleftarrows (\mathrm{H}^+)_p(\mathrm{MoO_4}^{2-})_q(\mathrm{C_6H_5PO_3}^{2-})_r$$

The complex on the right-hand side will simply be referred as (p,q,r) and its formation constant as $\beta_{p,q,r}$. In addition the following symbols will be used throughout the text.

H: hydrogen concentration over the chosen zero level; H_2O, MoO_4^{2-} and $C_6H_5PO_3^{2-}$
B: total concentration of MoO_4^{2-}
C: total concentration of $C_6H_5PO_3^{2-}$
h: free concentration of hydrogen ion in M
Z: average number of H^+ bound per MoO_4^{2-} ($Z = (H - h)/B$)
$Z_{B,C}$: average number of H^+ bound per $MoO_4^{2-} + C_6H_5PO_3^{2-}$ ($Z_{B,C} = (H - h)/(B + C)$)

Experimental Section

Chemicals. Phenylphosphonic acid (Aldrich) was dried under vacuum overnight. Sodium chloride (Merck, p.A.) was dried at 180 °C for 8 h.

(1) Throughout this work, the term "lg" stands for $\log_{10}$, one of three recommendations of the IUPAC Commission on Symbols, Terminology and Units [*Pure Appl. Chem.* **1979**, *51*, 24 (decadic logarithm of a: lg a, $\log_{10} a$, log a)]. The present work performed under constant ionic strength involves calibration of the glass electrode against the concentration of H^+. Thus we use $-\lg [H^+]$ rather than pH to distinguish our scale from the operationally defined NBS scale.
(2) Pettersson, L.; Andersson, I.; Öhman, L.-O. *Inorg. Chem.* **1986**, *25*, 4726.
(3) Hedman, B. *Acta Chem. Scand.* **1973**, *27*, 3335.
(4) Stalic, J. K.; Quicksall, C. O. *Inorg. Chem.* **1976**, *15*, 1577.
(5) (a) Kwak, W.; Pope, M. T.; Scully, T. F. *J. Am. Chem. Soc.* **1975**, *97*, 5735. (b) Sethuraman, P. R.; Leparulo, M. A.; Pope, M. T.; Zonnevijlle, F.; Brévard, C.; Lemerle, J. *J. Am. Chem. Soc.* **1981**, *103*, 7665.

†The University of Tokyo.
‡University of Umeå.

0020-1669/87/1326-3926$01.50/0

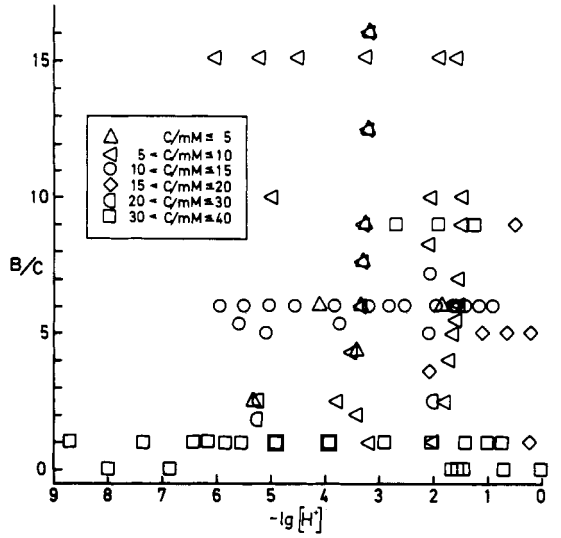

Figure 1. B/C ratios and acidities of the solutions whose ^{31}P NMR spectra were recorded. Different symbols are used for different ranges of C.

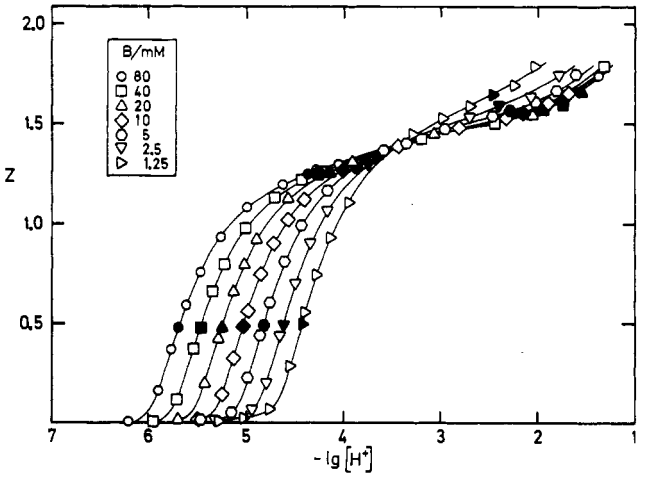

Figure 2. Average number of H^+ bound per MoO_4^{2-}, Z, as a function of $-\lg h$ ($=-\lg [H^+]$). Open symbols are from titrations at constant B and varying $[H^+]$ and filled symbols from titrations at almost constant Z and varying B. Solid lines are calculated by using the constants given in Table I.

Dilute hydrochloric acid (Merck, p.A.) was standardized against tris(hydroxymethyl)aminomethane (TRISMA-base). Stock solutions of $Na_2MoO_4 \cdot 2H_2O$ (Merck, p.A.) were prepared and analyzed as described earlier.[6]

Emf Measurements. The measurements were carried out as a series of potentiometric titrations in 0.6 M Na(Cl) medium at 25 °C with an automated potentiometric titrator, somewhat modified from the description given in ref 7. The glass electrodes, Ingold 201-NS, were tested against a hydrogen electrode and were found to give reliable values up to $-\lg h = 9.0$. The constant E_0 was determined separately in solutions with known hydrogen ion concentration before and after each titration.

NMR Measurements. ^{31}P NMR spectra were recorded on a Bruker WM-250 spectrometer in the same manner as described elsewhere.[2] All measurements were performed at 295 ± 1 K with broad-band proton irradiation in order to decouple spectra. The spin–lattice relaxation times (T_1) were evaluated by the inversion-recovery method. In order to obtain reliable quantitative data, 90° pulses and pulse repetition times larger than 5 times the longest T_1 were used.

Computer Programs. The mathematical analysis of emf data was performed with the least-squares program LETAGROPVRID, version ETITR.[8] Calculations and plotting of distribution diagrams were performed by using the program SOLGASWATER.[9] These computations were carried out on a CD Cyber 180-850 system. The combined emf–NMR data were analyzed with our new program LAKE[10] on a Cromemco System 300 computer. This program calculates formation constants and their standard deviations from NMR peak intensities and/or emf data (BETA) and chemical shift values for each species together with the standard deviations from a δ vs $-\lg h$ plot (SHIFT ESTIMATE) and adjusts stepwise formation constants and the chemical shift values for homonuclear series (STEP CONSTANT). The program also calculates the squares sum of relative NMR residuals

$$U_{\mathrm{rel},j} = \sum_n \left(\frac{c_{j,\mathrm{calcd}} - c_{j,\mathrm{obsd}}}{c_{j,\mathrm{obsd}}} \right)^2$$

and its root mean $s(U_{\mathrm{rel},j}) = (U_{\mathrm{rel},j}/n)^{1/2}$ for each different peak. The symbols $c_{j,\mathrm{calcd}}$ and $c_{j,\mathrm{obsd}}$ stand for the calculated and observed concentrations of an NMR-active nucleus that gives rise to the jth peak, and n is the number of observations.

The routine BETA minimizes the quantity

$$U_{\mathrm{comb}} = \sum_i (H_{\mathrm{calcd}} - H_{\mathrm{exptl}})^2 + \sum_i \sum_j f_j^2 (c_{j,\mathrm{calcd}} - c_{j,\mathrm{obsd}})^2$$

with respect to the free concentrations and formation constants. H_{calcd} and H_{exptl} are the calculated and experimental hydrogen ion concentrations over the zero level, and f_j is the weighting factor for each different peak. The summation is over j different peaks and i different data points. It is also possible to minimize the quantity

$$U'_{\mathrm{comb}} = \sum_i (H_{\mathrm{calcd}} - H_{\mathrm{exptl}})^2 + \sum_i \sum_j f_j^2 U_{\mathrm{rel},j}$$

In the current investigation $f_j = 2$ was used for all the three peaks observed. This weighting factor made the two terms of U_{comb} the same magnitude and the first term of U'_{comb} negligible.

Emf Data. About 500 data points were collected for the ternary H^+–MoO_4^{2-}–$C_6H_5PO_3^{2-}$ system. The data covered the ranges $8.2 \geq -\lg h \geq 1.4$, $10 \leq B/\mathrm{mM} \leq 80$, $5 \leq C/\mathrm{mM} \leq 40$, and $1 \leq B/C \leq 16$. In most cases stable emf values were attained within 5 min. However, we found somewhat slow equilibria in the range $4 > -\lg h > 3$ when B/C was around 2.5.

^{31}P NMR Data. The B/C ratios and $-\lg h$ ranges covered in this investigation are illustrated in Figure 1. A total of 88 different spectra were measured.

Table I. Species and Formation Constants in the Binary H^+–MoO_4^{2-} System

(p,q,r)	$\lg \beta_{p,q,r}$	proposed formula	(p,q,r)	$\lg \beta_{p,q,r}$	proposed formula
(0,1,0)		MoO_4^{2-}	(10,7,0)	60.78	$H_2Mo_7O_{24}^{4-}$
(1,1,0)	3.39	$HMoO_4^-$	(12,8,0)	71.62	$Mo_8O_{26}^{4-}$
(2,1,0)	7.35	H_2MoO_4	(13,8,0)	73.38	$HMo_8O_{26}^{3-}$
(8,7,0)	52.42	$Mo_7O_{24}^{6-}$	(15,8,0)	76.34	$H_3Mo_8O_{26}^-$
(9,7,0)	57.23	$HMo_7O_{24}^{5-}$			

Results and Discussion

A. Binary Systems. Molybdate System. Although there exists some disagreement among different authors about some minor species and the species formed under very acidic conditions in the H^+–MoO_4^{2-} system,[11] all of the data available to date clearly indicate that the first polymeric species formed on acidification of MoO_4^{2-} solution is $Mo_7O_{24}^{6-}$.[12] This was also the case in our investigation of the system in 0.6 M Na(Cl) medium. A series of hepta- and octamolybdates together with monomeric species explained satisfactorily the whole range of data (see Figure 2). The numerical values of each formation constant are given in Table I.

In the range $-\lg h < 2$ the emf results were ambiguous. More work has to be done to really establish the polyanion speciation in this region. However, since (15,8,0) has only a limited range

(6) Pettersson, L. *Acta Chem. Scand.* **1971**, *25*, 1959.
(7) Ginstrup, O, *Chem. Instrum. (N.Y.)* **1973**, *4*, 141.
(8) Brauner, P.; Sillén, L. G.; Whiteker, R. *Ark. Kemi* **1969**, *31*, 365.
(9) Eriksson, G. *Anal. Chim. Acta* **1979**, *112*, 375.
(10) Ingri, N.; et al., to be submitted for publication.
(11) Tytko, K. H.; Beathe, G.; Cruywagen, J. J. *Inorg. Chem.* **1985**, *24*, 3132.
(12) Baes, C. F., Jr.; Mesmer, R. E. *The Hydrolysis of Cations*; Wiley: New York, 1976; pp 253–257.
(13) A guanidinium salt of $(C_6H_5P)_2Mo_5O_{21}^{4-}$ has been isolated at our department and the existence of the Mo_5O_{15} ring unit confirmed from X-ray diffraction measurements. The full report will be published in *Acta Crystallogr.*

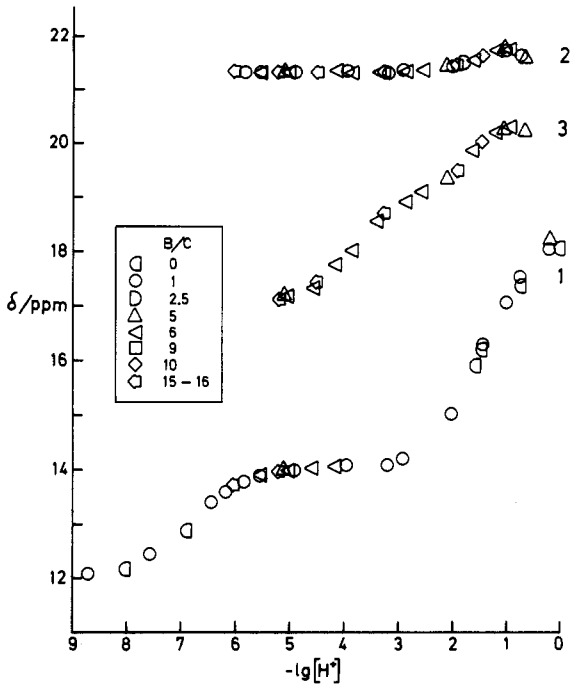

Figure 3. ^{31}P chemical shifts, δ, as a function of $-\lg h$ (=$-\lg [H^+]$).

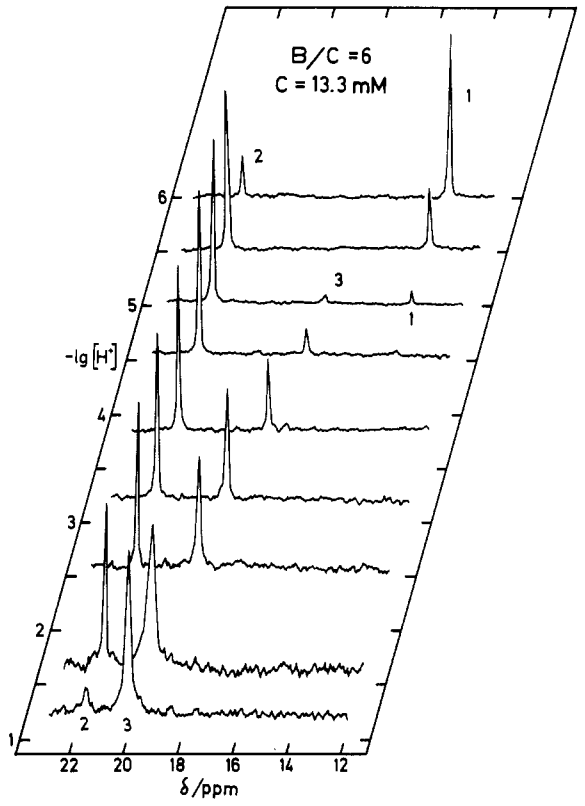

Figure 4. Typical spectra at $B/C = 6$. All spectra have been normalized to give the highest peak the same preset height.

of existence ($-\lg h < 2$), the final speciation of the ternary molybdophosphonate system would not be seriously affected by a change in the speciation of the pure molybdate system in very acidic solutions.

Phenylphosphonate System. Since there was no former report on the binary H^+–$C_6H_5PO_3^{2-}$ equilibria in 0.6 M Na(Cl), several separate titrations were performed to determine the formation constants of this system. A total of about 170 emf data points were collected. The data covered the ranges $8.7 \geq -\lg h \geq 1.6$ and $10 \leq C/\text{mM} \leq 40$. The titration curves, in the form $Z_c = f(-\lg h)$, did not show any sign of concentration dependence (see Figure 5a). This means that only monomeric species existed in the range investigated. Some ^{31}P NMR data of the pure binary phenylphosphonate system at $C = 40$ mM were also collected (symbol ▢ in Figure 3), but most NMR data were obtained from ternary solutions. The $-\lg [H^+]$ dependence of the chemical shift curve (number 1 in Figure 3) is in accordance with that of a diprotonated acid and the pK_a values determined agreed well with those calculated from emf data (see the following part). The results from the calculations are given in Tables II and XI and summarized in Table XII.

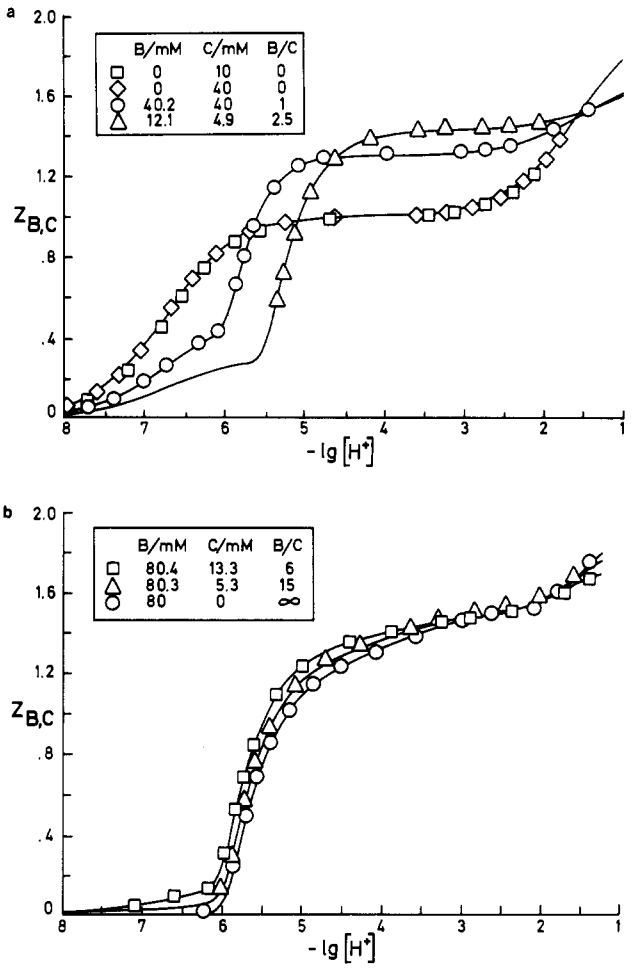

Figure 5. $Z_{B,C}$ $(H - h)/(B + C)$ as a function of $-\lg h$ (=$-\lg [H^+]$) at (a) low and (b) high B/C ratios. Solid lines are calculated by using the constants given in Tables I and XII.

Table II. Formation Constants, lg $\beta_{p,q,r}$ (3σ), of the Binary Phosphonate and Low-Ratio Ternary Species

	type of data, computer program			
	emf, LETAGROP		δ, LAKE (STEP CONSTANT)	peak int + emf, LAKE (BETA)
$-\lg [H^+]$ range	8.7–1.6	8.7–1.4	8.7–0.8	8.7–0.9
B/C	0	≤2.5	≤7.5	≤2.5
no. of points	172	181	75	21
lg $\beta_{p,q,r}$, peak 1				
(1,0,1)	6.71 (1)	6.71	6.73 (3)	6.72 (1)
(2,0,1)	8.26 (1)	8.26	8.26 (3)	8.32 (2)
lg $\beta_{p,q,r}$, peak 2				
(10,5,2)		68.07 (2)	68.07	68.05 (2)
(11,5,2)		69.50 (5)	69.50 (3)	69.34 (7)

B. Ternary System. In Figure 3, observed ^{31}P chemical shifts are shown as a function of $-\lg h$. Spectra at the ratio $B/C = 6$ are illustrated in Figure 4, showing all the three peaks observed

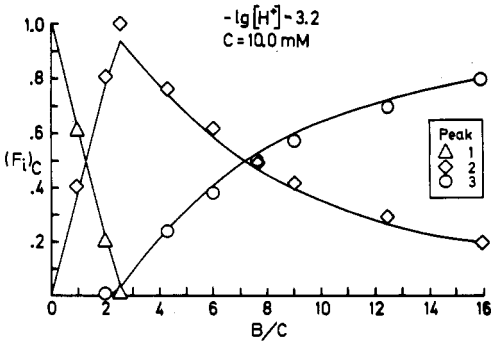

Figure 6. Relative peak intensities as a function of B/C. Solid lines are calculated by using the constants given in Tables I and XII.

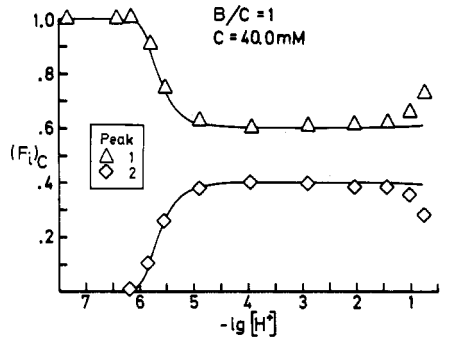

Figure 7. Relative peak intensities are $B/C = 1$ as a function of $-\lg h$ ($=-\lg [H^+]$). Solid lines are calculated by using the constants given in Tables I and XII.

Table III. Result of Testing Different Protonation Pairs on Emf Data of $5 \geq -\lg h \geq 3$ (106 Points)

species tested (p,q,r)	lg $\beta_{p,q,r}$ (3σ)	pK_a	av $p/(q+r)$	U/mM^2
(8,5,1)	53.26 (23)			
(9,5,1)	57.30 (15)	4.04	1.42	55
(9,5,1)	57.02		1.50	64
(10,5,1)	0	...		
(10,6,1)	64.93 (5)		1.50	8
(11,6,1)	67.71 (5)	2.78		
(11,7,1)	72.24 (5)		1.44	8
(12,7,1)	75.87 (4)	3.63		
(12,8,1)	78.71 (40)		1.39	43
(13,8,1)	83.71 (11)	5.00		
(13,8,1)	83.62 (9)		1.50	24
(14,8,1)	86.07 (14)	2.45		
(14,9,1)	91.02 (6)		1.45	10
(15,9,1)	94.43 (5)	3.41		
(15,10,1)	98.06 (18)		1.55	30
(16,10,1)	102.39 (10)	4.33		

in the current study. No additional peaks were observed even when the B/C ratio was increased to 16.

Low-Ratio Species. When $B/C \leq 2.5$, both emf and NMR data clearly showed the existence of only one ternary species over a wide $-\lg h$ range. Only one ternary NMR peak (peak 2) was observed at the low B/C ratios irrespective of $-\lg h$. Its chemical shift remained unchanged when $-\lg h$ was larger than 2.8. The potentiometric $Z_{B,C}$ vs $-\lg h$ curves at low B/C ratios showed plateaus over a relatively wide range of $-\lg h$ (Figure 5a). This means that at low B/C ratios almost all of the molybdate in solution is bound to this ternary species since the curves for the binary molybdate have no such plateau (Figure 2).

Figure 6 shows the result of a series of NMR measurements in which B/C was varied and $-\lg h$ was kept around 3.2. From this figure it can be deduced that the q/r ratio for the ternary species that gives rise to peak 2 is 2.5 and that peak 3 emanates from species having considerably higher q/r ratios. The relative peak intensities at $B/C = 1$ are plotted against $-\lg h$ in Figure 7. About 40% of the phosphonate in solution is bound to peak 2 species in the range $5 \geq -\lg h \geq 2$. This is totally consistent with the formation of one strong ternary complex of q/r ratio 2.5. As from Figure 5a the plateau for $B/C = 2.5$ has a $Z_{B,C}$ value somewhat higher than 1.4, the species $(H^+)_{10}(MoO_4^{2-})_5(C_6H_5PO_3^{2-})_2$ seems to be established ($10/(5+2) = 1.43$) although multiples cannot be ruled out.

Several heteropoly species of $q/r = 2.5$ were tested on the potentiometric data of $B/C \leq 2.5$. As expected, least-squares calculations showed that (10,5,2) explains the data best. However, the emf residuals showed some systematic error when we tried to explain these low-ratio data only by (10,5,2) in the very acidic region. Introduction of (11,5,2) to the system made the fit better.

Table IV. Result of Testing Different Protonation Series of Three Species on Emf Data of $5.2 > -\lg h > 1.8$ (154 Points)

species tested (p,q,r)	lg $\beta_{p,q,r}$ (3σ)	pK_a	U/mM^2
(10,6,1)	64.94 (6)		
(11,6,1)	67.62 (5)	2.68	21
(12,6,1)	0		
(11,7,1)	72.24 (7)		
(12,7,1)	75.83 (5)	3.59	16
(13,7,1)	77.67 (6)	1.84	
(12,8,1)	79.38 (15)		
(13,8,1)	83.60 (9)	4.22	27
(14,8,1)	86.40 (8)	2.80	
(14,9,1)	91.03 (8)		
(15,9,1)	94.36 (7)	3.33	22
(16,9,1)	96.50 (8)	2.14	

Table V. Residuals of Different Protonation Pairs on NMR Data of the Ranges $5.2 \geq -\lg h \geq 3.0$ and $B/C > 2.5$ (24 Points)

species tested (p,q,r)	lg $\beta_{p,q,r}$ (3σ)	pK_a	U'_{comb}	$s(U_{rel})$ peak 1	peak 2	peak 3
(10,6,1)	64.64 (5)					
(11,6,1)	67.62 (14)	2.98	3.48	0.14	0.13	0.13
(11,7,1)	71.80 (4)					
(12,7,1)	75.73 (3)	3.87	1.51	0.14	0.06	0.09
(12,8,1)	78.56 (6)					
(13,8,1)	83.51 (2)	4.76	1.43	0.14	0.06	0.09
(13,8,1)	83.59 (5)					
(14,8,1)	0.0	...	7.99	0.13	0.12	0.26
(14,9,1)	91.10 (5)					
(15,9,1)	94.11 (13)	3.01	3.43	0.14	0.13	0.12
(15,10,1)	98.15 (8)					
(16,10,1)	102.24 (6)	4.09	5.34	0.14	0.16	0.16

Table VI. Residuals of Different Protonation Series on NMR Data of the Ranges $5.2 \geq -\lg h \geq 2.0$ and $B/C > 2.5$ (31 Points)

species tested (p,q,r)	lg $\beta_{p,q,r}$ (3σ)	pK_a	U'_{comb}	$s(U_{rel})$ peak 1	peak 2	peak 3
(10,6,1)	64.69 (5)					
(11,6,1)	67.40 (19)	2.71	4.66	0.14	0.15	0.12
(12,6,1)	63.30 (98)	0.90				
(11,7,1)	71.80 (4)					
(12,7,1)	75.71 (3)	3.91	1.57	0.13	0.06	0.08
(13,7,1)	77.19 (21)	1.48				
(12,8,1)	78.84 (6)					
(13,8,1)	83.36 (5)	4.52	2.46	0.14	0.09	0.10
(14,8,1)	86.28 (6)	2.92				
(14,9,1)	91.11 (5)					
(15,9,1)	94.00 (19)	2.89	5.76	0.14	0.17	0.12
(16,9,1)	96.91 (60)	2.91				

Table VII. Residuals of Different Models on NMR Data of the Ranges $5.2 \geq -\lg h \geq 0.8$ and $B/C > 2.5$ (44 Points)

species tested (p,q,r)	lg $\beta_{p,q,r}$ (3σ)	pK_a	U'_{comb}	$s(U_{rel})$ peak 1	peak 2	peak 3
(11,7,1)	71.83 (13)					
(12,7,1)	75.63 (12)	3.80	38.21	0.14	0.45	0.11
(13,7,1)	77.96 (11)	2.33				
(12,8,1)	78.96 (22)					
(13,8,1)	82.81 (54)	3.85	107.30	0.14	0.76	0.18
(14,8,1)	86.79 (13)	3.98				
(11,7,1)	71.81 (5)					
(12,7,1)	75.70 (4)	3.89	5.43	0.14	0.15	0.08
(10,5,1)	58.84 (5)					
(11,7,1)	71.81 (5)					
(12,7,1)	75.70 (4)	3.89	4.74	0.14	0.14	0.07
(12,6,1)	69.11 (5)					
(12,8,1)	78.77 (7)					
(13,8,1)	83.51 (3)	4.74	3.88	0.14	0.12	0.07
(10,5,1)	58.94 (3)					
(12,8,1)	78.73 (10)					
(13,8,1)	83.54 (4)	4.81	6.84	0.14	0.18	0.08
(12,6,1)	69.23 (4)					

Table VIII. Results of the Combined Emf–NMR Calculations on the Data of $B/C > 2.5$ and $5.2 \geq -\lg h \geq 3.0$ (24 Points)

species tested (p,q,r)	lg $\beta_{p,q,r}$ (3σ)	pK_a	U_{comb}/ mM^2	$s(U_{rel})$ peak 1	peak 2	peak 3
(10,6,1)	64.64 (5)					
(11,6,1)	67.62 (9)	2.98	24	0.12	0.12	0.13
(11,7,1)	71.88 (5)					
(12,7,1)	75.68 (2)	3.80	15	0.13	0.06	0.13
(12,8,1)	78.75 (19)					
(13,8,1)	83.51 (2)	4.76	28	0.13	0.06	0.08
(13,8,1)	83.50 (5)					
(14,8,1)	85.79 (31)	2.29	41	0.13	0.10	0.29
(14,9,1)	90.95 (6)					
(15,9,1)	94.27 (6)	3.32	33	0.13	0.13	0.16
(15,10,1)	98.13 (14)					
(16,10,1)	102.23 (4)	4.10	58	0.14	0.16	0.17
(12,8,1)	78.89 (12)					
(13,8,1)	83.41 (5)	4.52	15	0.13	0.07	0.12
(14,8,1)	86.07 (13)	2.66				
(12,8,1)	78.92 (10)					
(13,8,1)	83.33 (5)	4.41	12	0.13	0.06	0.12
(11,6,1)	67.57 (11)					
(13,9,1)	85.71 (32)					
(14,9,1)	90.89 (8)	5.16	29	0.13	0.12	0.13
(15,9,1)	94.28 (6)	3.39				
(14,9,1)	90.21 (4)					
(15,9,1)	0		18	0.13	0.07	0.16
(11,6,1)	67.81 (5)					
(13,9,1)	85.74 (22)					
(14,9,1)	90.89 (4)	5.15	13	0.13	0.06	0.09
(11,6,1)	67.83 (5)					
(13,9,1)	85.69 (21)					
(14,9,1)	90.71 (11)	5.01	11	0.13	0.06	0.09
(10,6,1)	64.12 (22)					
(11,6,1)	67.78 (5)	3.66				
(15,10,1)	98.29 (6)					
(16,10,1)	101.45 (21)	3.16	20	0.14	0.08	0.12
(11,6,1)	67.87 (8)					

Slight changes in chemical shift of peak 2 in the low $-\lg h$ region (Figure 3) also indicates protonation of (10,5,2).

Formation constants of (10,5,2) and (11,5,2) based on the same emf data mentioned above are given in Table II together with those obtained from NMR data. The routine STEP CONSTANT gave virtually the same constants as those obtained from emf data for both ternary and binary phosphonic species. The two most acid peak 2 points in Figure 3 have been excluded in the calculations, their chemical shift values being unreliable due to extremely low intensity. Although the routine BETA gave slightly different constants for (11,5,2) and (2,0,1), we can conclude that the results of the three calculations shown in Table II agree well with each other considering the difficulty in determining $-\lg h$ accurately

Table IX. Results of the Combined Emf–NMR Calculations on the Data of $B/C > 2.5$ and $5.2 \geq -\lg h \geq 2.0$ (34 Points)

species tested (p,q,r)	lg $\beta_{p,q,r}$ (3σ)	pK_a	U_{comb}/ mM^2	$s(U_{rel})$ peak 1	peak 2	peak 3
(10,6,1)	64.71 (4)					
(11,6,1)	67.32 (5)	2.61	75	0.12	0.14	0.16
(12,6,1)	0					
(11,7,1)	71.91 (6)					
(12,7,1)	75.64 (3)	3.73	23	0.12	0.06	0.14
(13,7,1)	77.34 (9)	1.70				
(12,8,1)	78.94 (12)					
(13,8,1)	83.36 (3)	4.42	28	0.13	0.08	0.12
(14,8,1)	86.22 (3)	2.86				
(11,7,1)	71.90 (6)					
(12,7,1)	75.67 (2)	3.77	25	0.13	0.06	0.14
(12,6,1)	68.88 (10)					
(12,8,1)	78.85 (16)					
(13,8,1)	83.42 (3)	4.57	41	0.13	0.07	0.12
(11,6,1)	67.33 (4)					
(12,6,1)	0					
(12,8,1)	78.94					
(13,8,1)	83.33 (3)	4.39	23	0.13	0.07	0.12
(14,8,1)	86.06 (12)	2.73				
(11,6,1)	66.90 (28)					
(13,9,1)	85.71					
(14,9,1)	90.90 (6)	5.19	40	0.13	0.09	0.12
(15,9,1)	94.12 (8)	3.22				
(11,6,1)	67.29 (7)					
(15,10,1)	98.17 (12)					
(16,10,1)	102.11 (5)	3.94	68	0.14	0.13	0.15
(11,6,1)	67.39 (5)					
(12,6,1)	0					

Table X. Results of the Combined Emf–NMR Calculations on the Data of $B/C > 2.5$ and $5.2 \geq -\lg h \geq 0.8$ (43 Points)

species tested (p,q,r)	lg $\beta_{p,q,r}$ (3σ)	pK_a	U_{comb}/ mM^2	$s(U_{rel})$ peak 1	peak 2	peak 3
(11,7,1)	71.91					
(12,7,1)	75.68 (5)	3.77	224	0.13	0.36	0.13
(13,7,1)	77.23 (18)	1.55				
(14,7,1)	79.12 (6)	1.89				
(11,7,1)	71.89 (7)					
(12,7,1)	75.67 (2)	3.78	64	0.13	0.14	0.10
(13,7,1)	0					
(12,6,1)	69.02 (2)					
(12,8,1)	78.94					
(13,8,1)	83.42 (4)	4.48				
(14,8,1)	86.07 (5)	2.65	101	0.13	0.20	0.11
(11,6,1)	0					
(12,6,1)	69.13 (3)					
(13,9,1)	85.71					
(14,9,1)	90.90	5.19				
(15,9,1)	94.28 (5)	3.38	88	0.13	0.19	0.09
(11,6,1)	66.99 (13)					
(12,6,1)	69.07 (3)	2.08				
(15,10,1)	98.29					
(16,10,1)	102.14 (5)	3.85	115	0.15	0.18	0.11
(11,6,1)	67.26 (6)					
(12,6,1)	68.93 (4)	1.67				
(14,9,1)	90.78 (7)					
(12,7,1)	75.67 (3)		78	0.13	0.14	0.15
(12,6,1)	69.04 (2)					

Table XI. Comparison of the lg $\beta_{p,q,r}$ (3σ) Values Obtained from Different Calculations[a,b]

		type of data, computer program									
		emf, LETAGROP		peak int, LAKE (BETA)		peak int + emf, LAKE (BETA)		δ, LAKE (STEP CONSTANT)	final model		
lg $\beta_{p,q,r}$											
peak 1	(1,0,1)	6.71	[6.71]	6.71	[6.71]	6.72	[6.72]	[6.73 (3)]	6.71 (1)	[6.71]	
	(2,0,1)	8.26	[1.55]	8.26	[1.55]	8.32	[1.60]	[1.53 (3)]	8.26 (2)	[1.55]	
peak 2	(10,5,2)	68.07		68.07		68.07 (1)			68.07 (2)		
	(11,5,2)	69.48 (4)	[1.41]	69.50	[1.43]	69.34 (5)	[1.27]	[1.43 (3)]	69.40 (10)	[1.33]	
peak 3	(11,7,1)	72.11 (4)		71.81 (5)		71.90 (6)			71.96 (9)		
	(12,7,1)	75.73 (4)	[3.62]	75.70 (4)	[3.89]	75.69 (2)	[3.79]	[3.79 (2)]	75.70 (4)	[3.74]	
	(12,6,1)	69.02 (4)		69.11 (5)		69.05 (2)			69.04 (5)		
U/mM^{2}[c]		81		180		110			105		
$s(U_{rel})$[d]											
peak 1		0.09		0.08		0.08			0.08		
peak 2		0.16		0.13		0.12			0.13		
peak 3		0.29		0.07		0.10			0.15		

[a] When no 3σ value is given, the lg $\beta_{p,q,r}$ value was fixed in the calculation. [b] The pK_a's are given in brackets. [c] Calculated for 543 emf data points. [d] Calculated for 57 NMR data points.

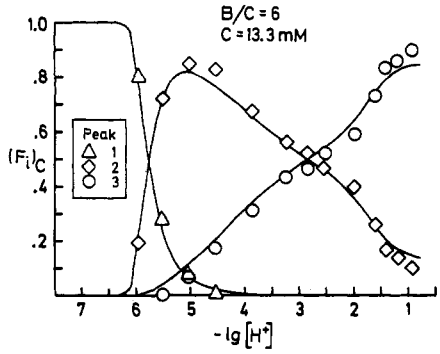

Figure 8. Relative peak intensities at $B/C = 6$ as a function of $-\lg h = -\lg [H^+]$). Solid lines are calculated by using the constants given in Tables I and XII.

for very acidic solutions and the low S/N ratio for many spectra of low $-\lg h$ solutions.

The values obtained from the pure emf data were used throughout the following work for the high-ratio species.

High-Ratio Species. Peak 3 in Figure 3 originates from the high-ratio species, and the chemical shift curve indicates the formation of three such species. By restriction of the acidity range to $-\lg h > 3$ the most acid complex can be excluded in the search. We thus carried out a (p,q,r) analysis on the emf data of $5 \geq -\lg h \geq 3$ and $B/C > 2.5$ by testing proton pairs. Low error squares sums were obtained for $q/r = 6$–9 and $p/(q + r) = 1.4$–1.5. However, the result was not decisive (see Table III). We then proceeded by extending the $-\lg h$ range and tested protonation series of three species. Again the result was not decisive (see Table IV). It was thus not possible to draw an unambiguous conclusion concerning the high-ratio species from the emf data alone. It only shows that so far as different species have similar $p/(q + r)$ values they give similar U values.

The next step in our search was to carry out lest-squares calculations on NMR data (peak intensities) in the range $5.2 \geq -\lg h \geq 3.0$. (U_{comb} was minimized.) The results are given in Table V. The $(p,8,1)$ and the $(p,7,1)$ series gave the "best" explanation of the peak intensity data. Although the $(p,8,1)$ series gave the lowest error squares sum, the pK_a value obtained for (13,8,1) differed 1 unit from that determined from the chemical shift curve, in contrast to that for (12,7,1), which was in accordance. Note that $(p,6,1)$, which gave as low an error squares sum as $(p,7,1)$ on the pure emf data (Table III), did not give very good results on the NMR data.

When we extended the $-\lg h$ range to 2.0 and tested protonation series of three, $(p,7,1)$ gave a better result than $(p,8,1)$ (see Table VI). The formation constants of (11,7,1) and (12,7,1) obtained were the same as those in Table V, while somewhat different values were obtained for (12,8,1) and (13,8,1). The large error of the (13,7,1) constant indicates a limited amount to be formed in this $-\lg$ range.

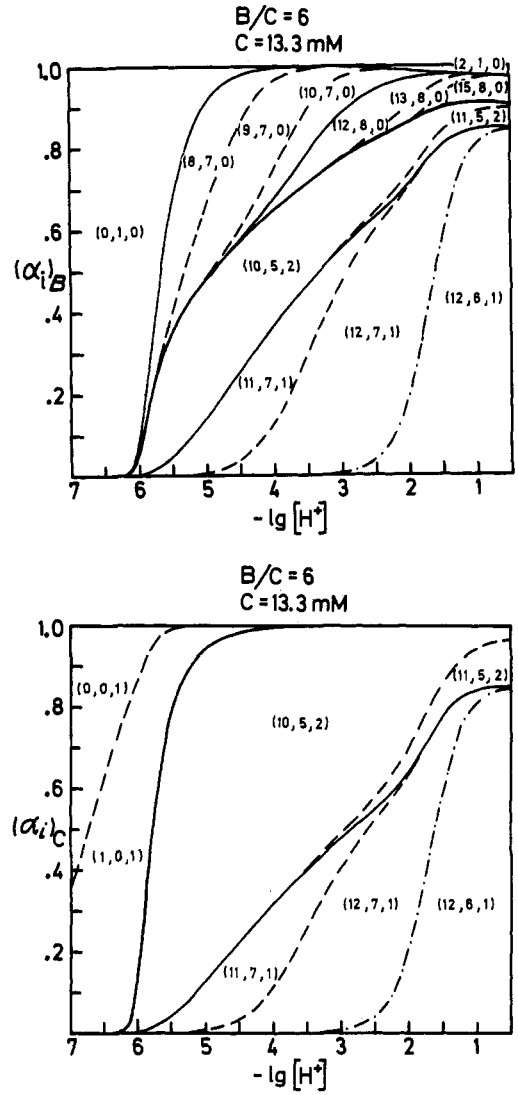

Figure 9. Calculated distribution of molybdenum (top) and phosphorus (bottom) among different species at $B/C = 6$. The quantity $(\alpha_i)_B$ ($(\alpha_i)_C$) is the ratio of molybdenum (phosphorus) bound in each species to the total amount. The constants given in Tables I and XII were used in the calculations.

Table XII. Summary of the Results

(p,q,r)	lg $\beta_{p,q,r} \pm 3\sigma$	pK_a	peak	$\delta \pm \sigma$	proposed formula
(0,0,1)			1	12.05 ± 0.05	$C_6H_5PO_3^{2-}$
(1,0,1)	6.71 ± 0.01	6.71		14.01 ± 0.02	$C_6H_5PO_2(OH)^-$
(2,0,1)	8.26 ± 0.02	1.55		17.68 ± 0.06	$C_6H_5PO(OH)_2$
(10,5,2)	68.07 ± 0.02		2	21.30 ± 0.01	$(C_6H_5P)_2Mo_5O_{21}^{4-}$
(11,5,2)	69.40 ± 0.10	1.33		22.02 ± 0.03	$(C_6H_5P)_2Mo_5O_{20}(OH)^{3-}$
(11,7,1)	71.96 ± 0.09		3	17.09 ± 0.05	$(C_6H_5P)Mo_7O_{25}(OH)^{5-}$
(12,7,1)	75.70 ± 0.04	3.74		19.15 ± 0.04	$(C_6H_5P)Mo_7O_{25}(H_2O)^{4-}$
(12,6,1)	69.04 ± 0.05			20.24 ± 0.05	$(C_6H_5P)Mo_6O_{21}(H_2O)_6^{2-}$

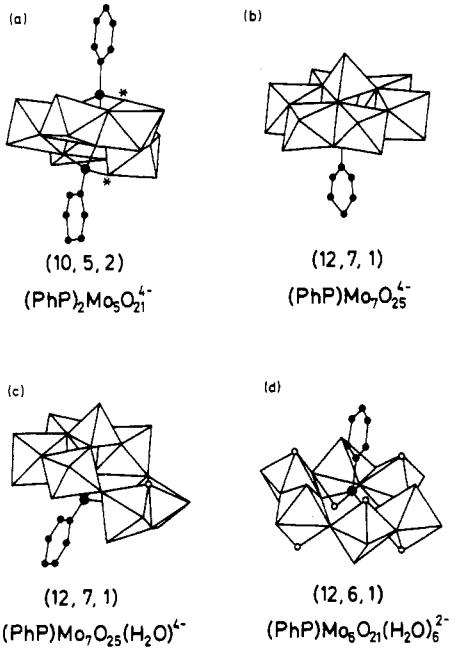

Figure 10. Possible structures of the species found in solution. PhP stands for C_6H_5P.

Although the results so far were in favor of $(p,7,1)$, they failed to explain the data of a wider $-\lg h$ range ($5.2 \geq -\lg h \geq 0.8$; see Table VII). The $(p,8,1)$ series, which gave the lowest error squares sum in the limited range of $5.2 \geq -\lg h \geq 3.0$, became even worse here. Stoichiometric calculations showed that the q/r ratio could not be 9 or higher in the range $-\lg h \geq 2$. In the most acidic region ($-\lg h < 1.6$) the ratio should be even lower than 7. Since it was not possible to explain the whole range of data with species having $q/r < 7$, it became apparent that some additional acidic low-q/r species was responsible for peak 3 together with $(p,7,1)$.

The search for this additional species was performed on the NMR data of $5.2 \geq -\lg h \geq 0.8$ and $B/C > 2.5$. The formation constants of (11,7,1) and (12,7,1) were fixed at the values given in Table VI. The species (12,6,1) came out to be the best and (10,5,1) the second best. A similar search was performed with $(p,8,1)$ instead of $(p,7,1)$. In this case (10,5,1) came out to be the best and (12,6,1) the second best. Further analysis was made by varying the formation constants of all the three species of possible combinations. The results are given in Table VII.

Although the combination of $(p,8,1)$ and (10,5,1) gave the lowest error squares sum, it could not reproduce the observed δ vs $-\lg h$ curve. It was not possible to explain the emf data with the combination of $(p,7,1)$ and (10,5,1). Only the combination of $(p,7,1)$ and (12,6,1) gave reasonably low error squares sums for both kinds of data.

Thus, for establishment of the final speciation, both emf and NMR data have to be taken into consideration. Another set of calculations was therefore carried out. Here the emf data for the NMR data points were used together with their peak intensity data. In the LAKE calculations the weighting factor f_j was applied so that both kinds of data contributed almost equally to the U_{comb} value. The results from the different $-\lg h$ ranges are given in Tables VIII–X. The combination of $(p,7,1)$ with (12,6,1) gave the lowest error squares sum irrespective of the $-\lg h$ range chosen. Several other combinations that seemed possible considering the q/r ratios and $p/(q+r)$ values were also tested. None of them gave a better explanation of the system. The results of several different calculations with (11,7,1), (12,7,1), and (12,6,1) as high-ratio species are compared in Table XI. Except for (11,7,1), basically the same formation constants were obtained. The calculation based on the pure emf data gave a somewhat larger $\beta_{11,7,1}$ constant. This might be caused by a small amount of impurity or some minor molybdate species that has a p/q value around 1.35. The final refinement of formation constants of all species containing phenylphosphonate was performed on both NMR and emf data.

The solid lines in Figures 5–8 show the calculated distribution with the final set of constants. These lines agree well with the experimental points. There is some systematic deviation in the very acidic region for $-\lg h < 1.5$, especially at $B/C = 1$ (Figure 7). We believe this deviation will disappear if cationic molybdate and/or higher nuclear isomolybdate species are introduced to the system. However, no further efforts were made to obtain a better fit between the observed and calculated distributions in this region.

Distribution. Figure 9 shows the molybdenum (top) and phosphorus (bottom) distribution at $B/C = 6$. These diagrams tell us that, in the current system, high-ratio species in the medium $-\lg h$ range, namely $(p,7,1)$, are quite weak. Notable amounts of isopolymolybdates exist even at such a low B/C ratio as 6, and the phosphonate bound in $(p,7,1)$ never exceeds 50% of the total amount. This weakness of $(p,7,1)$ is also shown in Figure 6. More than 20% of the phosphonate in solution is bound in $(p,5,2)$ even at such a high B/C ratio as 16. This makes a marked difference between the present system and its inorganic analogue. In the latter system no isopolymolybdate formation was observed when $B/C \lesssim 9$ due to the existence of strong high-ratio species, $(p,11,1)$ and $(p,9,1)$.

Solution Structure. Tentative formulas of the species found in solution are given in Table XII. The $(C_6H_5P)_2Mo_5O_{21}^{4-}$ anion has been characterized by UV and IR spectra and elemental analysis.[5a] An X-ray diffraction study of the anion is in progress at our department, and the structure given in Figure 10a has been confirmed.[13] Possible protonation sites are indicated by asterisks.[14] The $(PhP)_2Mo_5O_{21}^{4-}$ structure is as expected analogous to that of $(CH_3P)_2Mo_5O_{21}^{4-}$ and $(NH_3C_2H_4P)_2Mo_5O_{21}^{2-}$.[4]

Several structures are possible for (12,7,1). Klemperer et al.[15] have isolated $C_6H_5AsMo_7O_{25}^{4-}$ from MeCN solution and proposed the anion to have the structure shown in Figure 10b from their ^{17}O NMR measurements. It is possible to derive the structure of (12,7,1) from this proposed structure by simply substituting As with P. However, the resulting model does not give a simple explanation for (11,7,1), since the anion does not have a dissociable hydrogen atom. Jameson et al.[16] reported the structure of $CH_3AsW_7O_{27}H^{7-}$, but it is not likely that (11,7,1) and (12,7,1) have a directly related structure, because $CH_3AsW_7O_{27}H^{7-}$ is reported to be unstable in solution. The structure shown in Figure

(14) The calculation of the bond orders for several known Mo_5P_2 structures indicated the oxygens doubly shared by one Mo atom and one P atom are slightly more basic than the others.

(15) Klemperer, W. G.; Schwarts, C.; Wright, D. A. *J. Am. Chem. Soc.* **1985**, *107*, 6941.
(16) Jameson, G. B.; Pope, M. T.; Wasfi, S. H. *J. Am. Chem. Soc.* **1985**, *107*, 4911.

10c is most plausible for (12,7,1). This structure is closely related to the structure of $(C_6H_5As)_2Mo_6O_{25}H_2^{4-}$.[17] It has a tetrahedral Mo group instead of the second heteroatom group. The species (11,7,1) is then easily explained by the dissociation of one of the protons of the water molecule, which is indicated by an open circle in Figure 10c. If we remove the MoO_4^{2-} group from this structure and rearrange the atoms, it turns out to be the structure of (12,6,1), which is shown in Figure 10d. The $CH_3AsMo_6O_{21}(H_2O)_6^{2-}$ anion has been reported to have a similar structure.[18] The structures in Figure 10c,d are thus proposed as the solution structures for (12,7,1) and (12,6,1). Considering the fast exchange between the two species, even from an NMR point of view this pair seems credible.

Concluding Remarks

The results obtained in the system are summarized in Table XII. Although the speciation may seem rather simple, the establishing of the equilibrium model was very tedious and not at all straightforward. As mentioned before, an ordinary (p,q,r) search did not work well for the current system. Figure 5b explains the reason. The observed titration curves at B/C ratios 6 and 15 were quite similar, especially in the range $3.5 > -\lg h > 2$. Moreover, the $Z_{B,C}$ $(=(H-h)/(B+C))$ values in that range were very close to those of the binary molybdate system in the same range. This means that it is difficult to find whether an additional ternary species is formed in this region from emf data alone. Although potentiometry is a powerful tool for investigating solution equilibria, it thus gives an ambiguous result if two or more different species that consume about the same amounts of protons or other ions measured by the electrode are present in solution. This is often the case with polyoxometalates.

On the other hand, the NMR data alone could not lead us to the final model either. It is the combined emf–NMR technique that once again proved to be very powerful for establishing the equilibrium conditions in polyanion systems. It is thereby of vital importance that the NMR data are collected in a quantitative way.

This is the first time we have systematically tested emf and NMR data individually and then the combination. We have therefore chosen to report calculations from different B/C and $-\lg h$ ranges to illustrate all the relevant calculations performed for establishing the final model.

The LAKE program, capable of treating all kinds of information from the combined data, has proved to be very valuable. Although more work has to be done toward a proper way of weighting different kinds of data and different points, the method described in the current paper could be applied to numerous other systems successfully also.

Acknowledgment. We thank Professor Nils Ingri and Professor Yukiyoshi Sasaki for their great interest and valuable advice, the members of the NMR group at the Department of Organic Chemistry, Umeå University, for being in charge of the Bruker NMR apparatus, Christina Broman for typing the manuscript, and Lage Bodén for drawing the figures. This work forms part of a program financially supported by the Swedish Natural Science Research Council.

Registry No. MoO_4^{2-}, 14259-85-9; $C_6H_5PO_3^{2-}$, 16486-11-6.

(17) Matsumoto, K. Y. *Bull. Chem. Soc. Jpn.* **1978**, *51*, 492.
(18) A similar heteropolyanion has been found in the molybdate–methylarsonate system. See: Matsumoto, K. Y. *Bull. Chem. Soc. Jpn.* **1979**, *52*, 492.

Contribution from the Laboratorium für anorganische Chemie, ETH-Z, CH-8092 Zürich, Switzerland, and Istituto di Chimica Farmaceutica, Università di Milano, I-20131 Milano, Italy

Silver- and Gold-Containing Heterobinuclear Hydrido-Bridged Complexes

Alberto Albinati,[1a] Hans Lehner,[1b] Luigi M. Venanzi,*[1b] and Martin Wolfer[1b]

Received June 5, 1987

The hydrido-bridged complex cations $[(PR_3)_2(R')Pt(\mu\text{-}H)M(PR''_3)]^+$ (M = Ag: R = Et, R′ = C_6Cl_5, R″ = Et, *i*-Pr, Cy, and Ph; R = Me, R′ = C_6Cl_5, R″ = *i*-Pr and Cy. M = Au: R = Et, R′ = C_6Cl_5, R″ = *i*-Pr and Ph; R = Et, R′ = C_6F_5, and R″ = Ph; R = Et, R′ = Ph, R″ = Ph; R = *i*-Pr, R′ = Ph, R″ = Ph) were prepared from the corresponding *trans*-$[PtH(R')(PR_3)_2]$ and $[M(solv)(PR''_3)]^+$ (solv = THF, Et_2O) complexes. Their ^1H and ^{31}P NMR data are reported together with ^{31}P data for the complexes $[Ag(PR''_3)_2]^+$. The X-ray crystal structure of $[(PEt_3)_2(C_6F_5)Pt(\mu\text{-}H)Au(PPh_3)](CF_3SO_3)$ was determined. Its structure is monoclinic, space group $P2_1/c$, with $Z = 4$, $a = 23.609$ (5) Å, $b = 9.725$ (4) Å, $c = 19.683$ (5) Å, and $\beta = 72.91$ (2)°. The final agreement factor (for the 3862 observed reflections) R is 0.043. The structure consists of *trans*-$[PtH(C_6F_5)(PEt_3)_2]$ and "$Au(PPh_3)^{+}$" units held together by the hydride ligand and a Pt–Au bond.

Introduction

Although several homometallic copper(I) hydrides are known,[2] the corresponding compounds of silver and gold do not appear to have been reported in the literature. However, Wiberg and Henle[3] describe the isolation of $Ag[BH_4]$ and $Ag[AlH_4]$, which decompose at temperatures above −30 and −50 °C, respectively. This ease of decomposition is probably associated with the high oxidation potential of silver ($Ag^+ + e^- \rightarrow Ag$, 0.80 V).[4] Attempts to prepare AuH_3, $Au[AlH_4]$, and $Au[BH_4]$ gave products that decompose above −120 °C.[5] Furthermore, the reactions of complexes $[AuX(PR_3)_n]$ with $Na[BH_4]$ produce gold clusters that do not contain hydridic ligands.[6]

As shown by several research groups,[7] unstable mononuclear transition metal hydrides, L_mMH_x, can often be stabilized by "coordinating them" to a coordinatively unsaturated metal complex, $M'L'_n$, i.e., by forming species of the type $L_mM(\mu\text{-}H)_xM'L'_n$. Thus, Green et al.[8] reported the isolation of complexes of the types $[(CO)_5M(\mu\text{-}H)M'(PR_3)]$ (M = Cr, Mo, W; M′ = Ag, Au; R = Ph, Me), while Lehner et al.[9] described the preparation of cationic species of the types $[(PPh_3)_3H_2Ir(\mu\text{-}H)Au(PR_3)]^+$ (R = Ph, Et) and $[(PEt_3)_2(C_6Cl_5)Pt(\mu\text{-}H)Au(PEt_3)]^+$ as well as the analogous silver compounds.[10] Since then, many silver- or gold-containing

(1) (a) Università di Milano. (b) ETH Zürich.
(2) (a) Churchill, M. R.; Bezman, S. A.; Osborn, J. A.; Wormald, J. *Inorg. Chem.* **1972**, *11*, 1818. (b) Caulton, K. G. *Ann. N.Y. Acad. Sci.* **1983**, *415*, 27. (c) Lemmen, T. J.; Folting, K.; Huffman, J. C.; Caulton, K. G. *J. Am. Chem. Soc.* **1985**, *107*, 7774.
(3) Wiberg, E.; Henle, W. *Z. Naturforsch. B: Anorg. Chem., Org. Chem., Biochem., Biophys., Biol.* **1952**, *7B*, 757.
(4) Latimer, W. M. *Oxidation Potentials*; Prentice-Hall: New York, 1952; p 343.
(5) Wiberg, E.; Neumaier, H. *Inorg. Nucl. Chem. Lett.* **1965**, *1*, 35.
(6) Malatesta, L. *Gold Bull.* **1975**, *8*, 48.
(7) Venanzi, L. M. *Coord. Chem. Rev.* **1982**, *43*, 251 and references quoted therein.
(8) Green, M.; Orpen, A. G.; Salter, I. D.; Stone, F. G. A. *J. Chem. Soc., Chem. Commun.* **1982**, 813.
(9) Lehner, H.; Matt, D.; Pregosin, P. S.; Venanzi, L. M.; Albinati, A. *J. Am. Chem. Soc.* **1982**, *104*, 6825.
(10) Lehner, H. *Dissertation* No. 7239, ETH Zürich, 1983.

0020-1669/87/1326-3933$01.50/0